Gibberellin-Induced Changes in Growth Anisotropy Precede Gibberellin-Dependent Changes in Cortical Microtubule Orientation in Developing Epidermal Cells of Barley Leaves. Kinematic and Cytological Studies on a Gibberellin-Responsive Dwarf Mutant, M489

Carol L. Wenzel[1], Richard E. Williamson, and Geoffrey O. Wasteneys*

Plant Cell Biology Group, Research School of Biological Sciences, Australian National University, G.P.O. Box 475, Canberra, Australian Capital Territory 2601, Australia

We conducted kinematic and cytological studies on "between vein" epidermal cells of the gibberellin (GA)-deficient M489 dwarf mutant of barley (*Hordeum vulgare* L. Himalaya). GAs affect radial and axial components of cell expansion and cortical microtubule orientation. Adaxial cells in particular expand radially after leaving the elongation zone (EZ), probably as part of leaf unrolling. Exogenous gibberellic acid corrects the mutant's short, wide blades, short EZ, and slow elongation rate. Cell production rates increase more on the adaxial than on the abaxial surface. Cells spend equal periods of time elongating in dwarf and tall plants, but relative elemental growth rates start to decline sooner in the dwarf. GA increased the rate at which longitudinal wall area increased because the increased axial growth more than compensated for reduced radial growth. In dwarf leaves, increased radial expansion was detected in basal parts of the EZ before cortical microtubules lost transverse orientation in the distal elongation zone. We conclude that loss of microtubule orientation is not required for low GA levels to reduce growth anisotropy.

Growth of cells in elongating plant organs is rarely uniaxial. No matter how highly anisotropic expansion may be, there is almost always significant, if minor, radial expansion accompanying at least part of the elongation phase. Increased radial expansion is associated with reduced longitudinal expansion in, for example, *Rht* dwarf wheat leaves, (Keyes et al., 1989; Tonkinson et al., 1995), in the temperature-sensitive radial swelling (Baskin et al., 1992) and conditional root expansion (Hauser et al., 1995) mutants of Arabidopsis, and in roots growing in compacted soil (Veen, 1982). Loss of transversely-aligned cortical microtubules (CMTs) also induces radial swelling and reduces axial growth, whether occurring naturally in onion bulb development (Mita and Shibaoka, 1983; Shibaoka, 1993) and potato tuberization (Fujino et al., 1995) or induced by chemicals (Srivastava et al., 1977; Durnam and Jones, 1982; Murata and Wada, 1989; Wasteneys, 1992). This effect is generally considered to relate to microtubules' involvement in aligning cellulose microfibrils. A plausible, but as yet unconfirmed, mechanism is by confining the movement of cellulose synthase complexes to regions of plasma membrane between adjacent parallel CMTs (Giddings and Staehelin, 1988, 1991).

Gibberellins (GAs) limit the extent of radial expansion in plant organs. Decreased axial growth and increased radial cell growth result from mutations or chemicals blocking GA biosynthesis (Tanimoto, 1987; Keyes et al., 1989; Barlow et al., 1991; Barlow, 1992; Baluska et al., 1993; Tonkinson et al., 1995) or from the *Rht*-wheat dwarfing allele, which confers GA insensitivity (Keyes et al., 1989; Tonkinson et al., 1995). GA effects on cell shape have been attributed to GAs aligning CMTs transversely to the long axis of growing cells (e.g. Mita and Shibaoka, 1984a; Mita and Katsumi, 1986; Shibaoka, 1993; Fujino et al., 1995), and low endogenous GA levels result in shorter, wider cells with non-transverse CMTs (e.g. Mita and Shibaoka, 1984b; Baluska et al., 1993). To date, however, few studies have measured radial expansion, loss of elongation, and CMT alignment with precision.

GA regulates leaf elongation in wheat (e.g. Tonkinson et al., 1995, 1997) and barley (*Hordeum vulgare* L. Himalaya; e.g. Chandler and Robertson, 1999). Exogenous gibberellic acid (GA_3) corrects leaf blade extension in M489, a GA-responsive dwarf mutant of barley. M489 has low endogenous levels of GA_1 and belongs to the complementation group defined by the *grd2* locus, which is thought to encode the GA 3β-hydroxylase (Chandler and Robertson, 1999; P.M. Chandler and J.R. Lenton, personal communication). In this paper we examine the effect of GA_3 on axial blade elongation, radial expansion, and CMT orientation in the M489 leaf blade, comparing the dwarf

[1] Present address: The Plant Lab, Biology Department, York University, York YO10 5DD, UK.

* Corresponding author; e-mail geoffw@rsbs.anu.edu.au; fax 61–2–6249–4331.

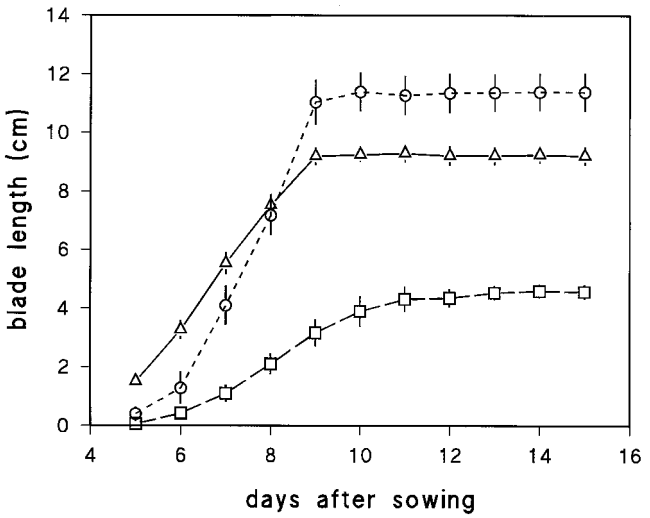

Figure 1. Blade length of leaf 1 plotted against time after sowing. Wild type (△), M489 dwarf (□), and M489 + GA_3 (○) (± SE, $n = 5$).

M489 plants with the tall barley (wild type and M489 + GA_3). We find that GA affects CMT alignment, but that altered radial expansion occurs before CMT changes are visible.

RESULTS

Reduced Axial Elongation in M489

The first leaf blade elongated for 9 d in tall plants (wild type and M489 + GA_3), but for 11 d in M489 (Fig. 1). We focused on the dynamics of cells in the elongation zone (EZ) of blades when they reached 50% of their final length and on the final size of the cells that left the EZ in the ensuing 24 h. The dwarf's blade elongation rate when one-half-grown was less than one-half the rate in the tall plants (Fig. 1; Table I), and kinematic analyses show why. Figure 2 illustrates similar rises in REGR in the basal part of all EZs, but earlier declines in the dwarf's REGR both in space (Fig. 2a) and in time (Fig. 2b). The time to transit the shorter M489 EZ was similar to the times to transit the longer EZs of tall barley leaves (Fig. 2b). There were major differences in the cell flux rates and cellochrons for abaxial and adaxial cells, but M489 had lower cell flux and higher cellochron values for both surfaces (Table I). The differences between the two surfaces meant that changes in final cell lengths on the abaxial surface of M489 were much greater than those on the adaxial surface.

Increased Radial Expansion in M489

Within the EZ of one-half-grown blades, the cross-sectional perimeters of abaxial cells increased more rapidly with distance in M489 and remained greater than the perimeters in the tall barleys (Fig. 3a). In contrast, the perimeters of M489 adaxial cells were not larger when they left the EZ (Fig. 3b). Both cell types, however, continued radial expansion after leaving the EZ, a zone conventionally defined on the basis of axial expansion alone. This was particularly pronounced in adaxial cells (Fig. 3b), but on both surfaces the final cell perimeters were M489 > wild type > M489 + GA, which parallels the final blade widths (Fig. 4).

Radial Expansion Does Not Fully Compensate Reduced Axial Expansion in M489

If GA simply adjusts the balance between radial and longitudinal wall extension, then in the simplest case, total wall area would not change. The total area of longitudinal wall added by cells leaving the EZ in that 24-h period can be calculated as the product of mature cell perimeter measured in 2-week-old blades and the 24-h increment in blade length (Table II). M489 gained less than one-half the longitudinal wall area gained by the tall barleys (Table II). Because fewer cells left the EZ of M489 in that period, however, there was no decline in the final surface area of each individual adaxial cell and the reduced abaxial cell area was less than the reduced total longitudinal wall area added during the 24-h period (Table I).

GA Maintained Transverse CMTs of Epidermal Cells for Most of the EZ

Epidermal CMT orientations varied along the length of the EZ, producing three regions of CMT

Table I. *Kinematic and cell size data for adaxial and abaxial "between the vein" epidermal cells in half-grown first leaves of barley (±SE; n = sample size)*

Growth Parameter	Leaf Surface	Wild Type	M489	M489 + GA_3
Blade elongation rate v (mm h^{-1})		1.04	0.44	1.28
Final cell length l_{max} (mm) (n = 5–7)	Adaxial	0.252 ± 0.003	0.229 ± 0.007	0.242 ± 0.004
	Abaxial	1.40 ± 0.01	0.90 ± 0.03	1.51 ± 0.01
Cell flux (h^{-1})	Adaxial	4.13	1.92	5.29
	Abaxial	0.74	0.49	0.85
Cellochron (h)	Adaxial	0.24	0.52	0.19
	Abaxial	1.34	2.05	1.18
Mature cell perimeter (mm) (n = 5)	Adaxial	0.132 ± 0.003	0.155 ± 0.003	0.119 ± 0.002
	Abaxial	0.123 ± 0.003	0.138 ± 0.003	0.102 ± 0.002
Mature cell surface area (mm^2)	Adaxial	0.033	0.035	0.029
	Abaxial	0.172	0.124	0.154

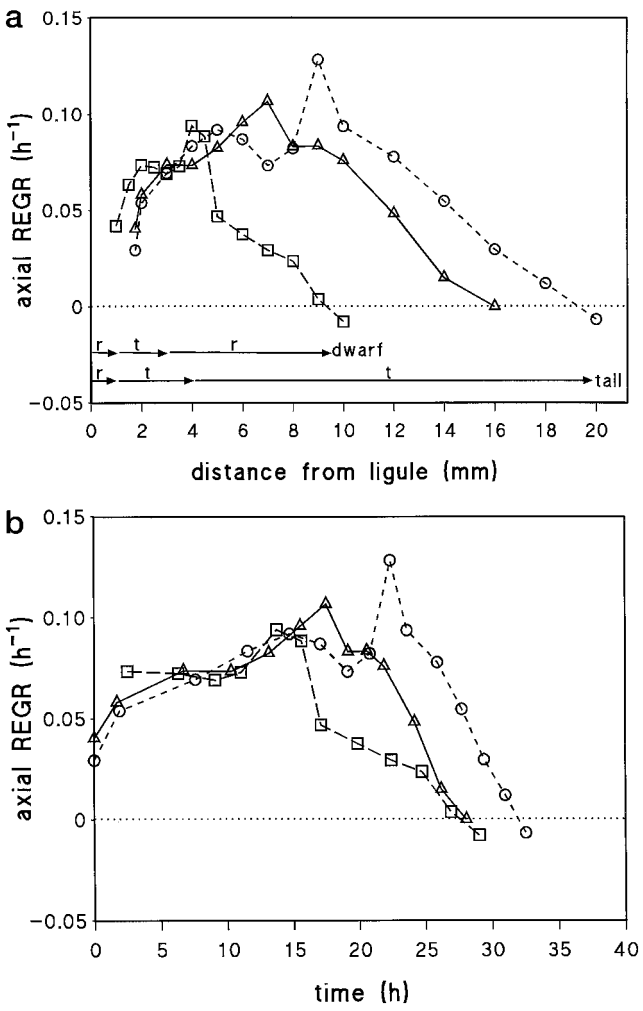

Figure 2. Axial relative elemental growth rate (REGR) plotted against distance from ligule (a) or developmental time (b; time zero is 1.75 mm from ligule) for abaxial cells of wild type (△), M489 (□), and M489 + GA_3 (○). Arrows in a summarize the orientations of the CMTs (r, random; t, transverse) at the corresponding positions throughout the EZ of the dwarf and tall plants.

orientation: meristematic (CMTs highly variable, from transverse through random to longitudinal), basal EZ (mostly transverse), and distal EZ (mostly disorganized in dwarf, transverse in tall barley). Dwarf and tall barley CMT orientations only diverged in the distal EZ. Despite differences in cell expansion dynamics for the two epidermal cell types (adaxial versus abaxial), no differences were evident in their CMT orientations. CMTs could not be labeled beyond the EZ.

Meristematic Zone

Preprophase bands (PPBs), spindle fibers, and phragmoplast microtubules were seen within 1 mm of the ligule (Fig. 5, b and c). Most cells in dwarf and tall barleys had variably-oriented CMTs ranging from transverse through random to occasionally longitudinal. Only 30% to 40% of the cells had predominantly transverse CMTs with most, but not all, resolved CMTs approximately transverse (Fig. 5, a–c). Adjacent cells often showed contrasting CMT orientations.

Basal EZ

Basal parts of the EZ, like the meristem, again showed no obvious differences in CMT orientation between dwarf and tall barleys. CMTs were predominantly transverse in ≥80% of all cells (excluding those associated with stomatal rows) for the basal approximately 1 to 3 mm of the dwarf and 1 to 4 mm

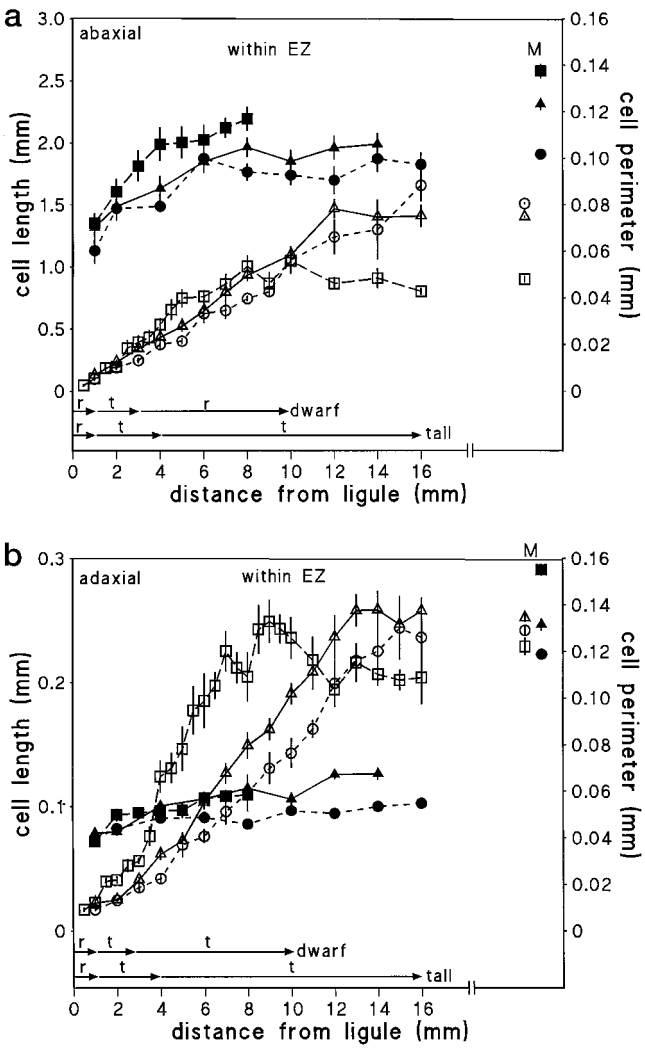

Figure 3. Cell length (white symbols) and cross-sectional cell perimeter (black symbols) plotted against distance from the ligule for abaxial (a) and adaxial (b) cells of wild type (△), M489 dwarf (□), and M489 + GA_3 (○) (± SE, n = 9). Cell perimeters were measured throughout the EZ of 50%-elongated blades (n = 9, ± SE) and mature perimeters were measured in fully grown leaves (n = 36, ± SE). Arrows summarize the orientation of CMTs (r, random; t, transverse) at the corresponding positions throughout the EZ of the dwarf and tall plants.

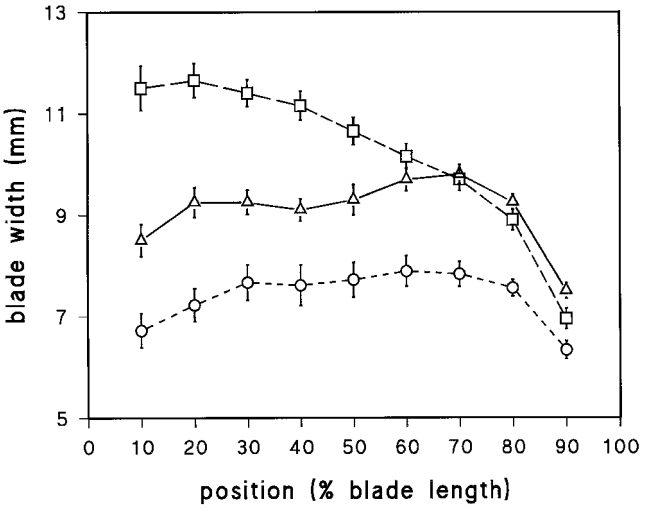

Figure 4. Blade width (± SE, $n = 10$) plotted against distance along leaf 1 with the ligule at 0% and the tip at 100%; wild type (△), M489 dwarf (□), and M489 + GA_3 (○)

of the tall barley (Fig. 5, d–f). It is important to note that CMTs were still predominantly transverse within the basal EZ of the M489 dwarf, despite significant radial expansion during this phase (Fig. 3). There was no obvious abrupt transition from the meristematic region (variable CMT orientations) to the basal EZ (predominantly transverse CMTs).

Distal EZ

CMT alignments diverged for the first time in this region, which extends about 4 to 8 mm from the ligule in M489 and 5 to 15 mm in the tall barleys. About 90% of cells in the wild type and 70% to 80% in M489 + GA had transverse CMTs (Figs. 6, a and b), whereas only about 30% of cells in M489 had what could be characterized as "loosely" transverse CMTs (Fig. 6d). The remaining cells (about 10% in wild type, 20%–30% in M489 + GA_3, and 70% in M489) had disordered CMTs (e.g. Fig. 6, c and e). CMT orientations could vary along the length of a single cell (Fig. 6f) or on different sides of the same cell (Fig. 6g). The percentage of labeled cells declined in the distal EZ and was generally zero beyond the EZ.

Interstomatal Cells

Interstomatal epidermal cells had transverse CMTs in the meristematic zone (Wenzel, 1998), but in basal and distal regions of the EZ, their CMTs were randomly oriented (Fig. 5,g–i). In the basal EZ, CMTs also coalesced to form transverse bands, consistent with a subsequent constraint of expansion in the middle region of the guard mother cells (Fig. 5, g and h), PPBs, which outline the guard cell division site (not shown), and PPBs in lateral cells, which outlined the lateral subsidiary cell division sites (Fig. 5, g and h). Once lateral subsidiary cells formed, the lateral cells developed transversely oriented CMTs (Wenzel, 1998).

Mesophyll Cells

There were no obvious differences between the dwarf and tall barleys. CMTs in mesophyll cells changed from being variously oriented to transverse at approximately 0.5 mm from the ligule (Fig. 6, h and i), sooner than the transition in epidermal cells. Mesophyll cells had randomly oriented CMTs with localized MT bands in cells approximately 2 to 4 mm from the ligule (Fig. 6j), but most cells >4 mm from the ligule had no MT bands in their random CMT arrays (Fig. 6k). The overlying epidermal cells (especially in tall barleys) had transverse CMTs (Fig. 6i). The development of MT bands is consistent with a role in providing localized constraint of expansion that results in lobing (see also Hellmann and Wernicke, 1998).

DISCUSSION

In this investigation we used a GA-deficient barley mutant to explore how GA controls growth and its polarity in epidermal cells. In particular we probed the relationship between CMT organization and the direction of cell expansion. We found that GA enhances axial expansion, suppresses radial expansion, and maintains transverse CMTs throughout the EZ, whereas CMTs were randomized in the distal EZ of the dwarf. Elongation, radial expansion, and CMT orientations, however, were not always closely coupled. In particular, despite CMTs remaining transverse, significant radial expansion occurs in the basal EZ when GA is lacking. This suggests that changes in growth anisotropy can begin without changes in CMT orientation. Although clearly necessary for anisotropic expansion, CMT transverse orientation appears to be insufficient for GA-mediated elongation.

Table II. *Additions in the 24 h after leaf 1 reached one-half its final length*

Addition	Leaf Surface	Wild Type	M489	M489 + GA_3
To blade length (mm)		25.0	10.6	30.8
To longitudinal wall area (mm^2)	Adaxial	3.29	1.64	3.66
	Abaxial	3.08	1.46	3.13
To cell number	Adaxial	99.21	46.29	127.27
	Abaxial	17.86	11.78	20.40

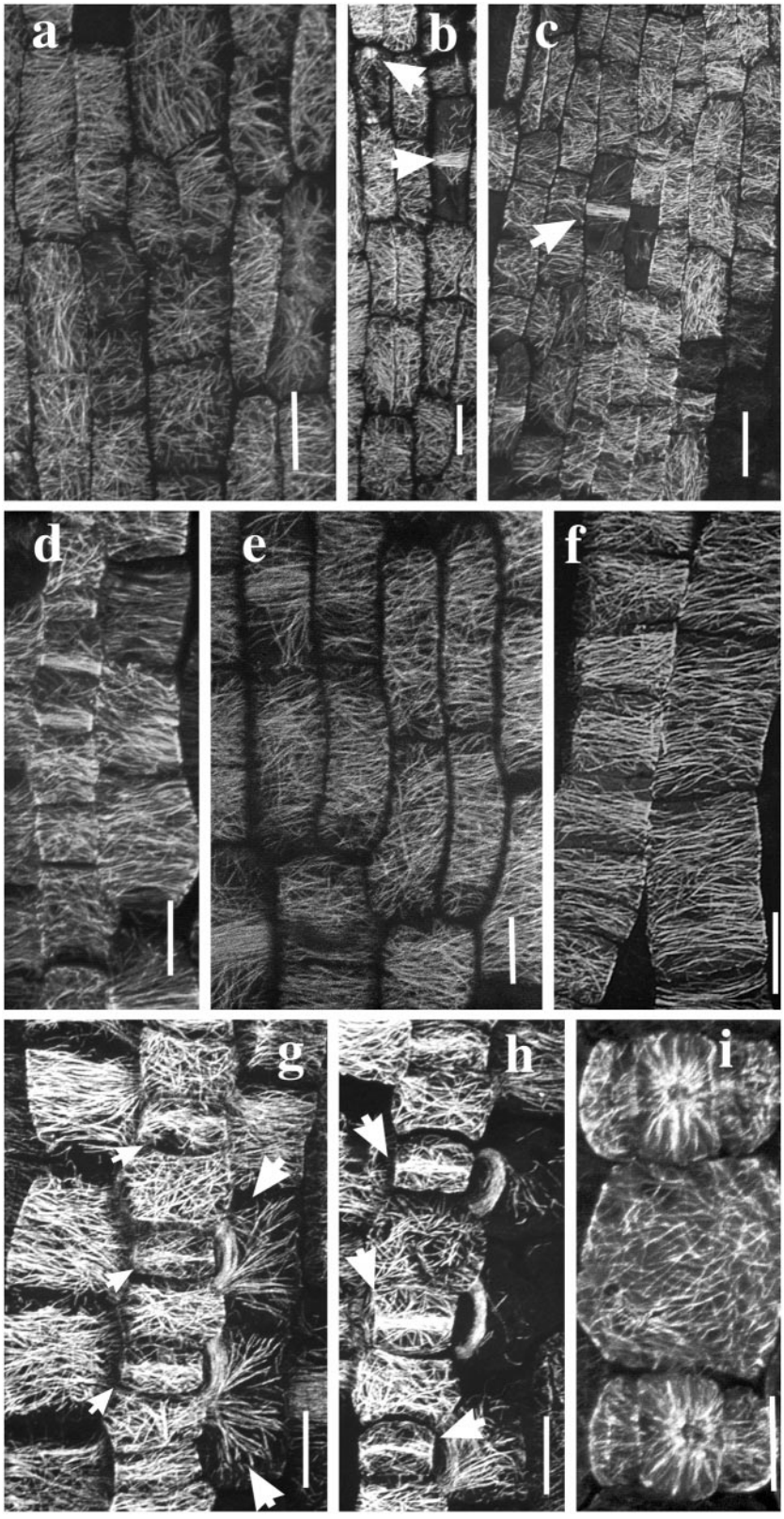

Figure 5. Confocal projections of immunofluorescently-labeled microtubules in cells of the meristematic zone (a–c), basal EZ (d–f), and the stomatal complexes (g–i) of barley leaf epidermis. In the meristematic region of wild type, 0 to 1 mm from ligule (a and b), CMT orientations ranged from predominantly transverse through random to longitudinal. Arrows in b indicate a transverse PPB and a longitudinal phragmoplast array. A similar range of microtubule patterns was observed in the equivalent region (0–1 mm from ligule) of the M489 dwarf (c). The arrow in c indicates a PPB. In the basal EZ, 2 to 5 mm from the ligule, CMTs in elongating epidermal cells were predominantly transverse. CMT patterns were similar in wild type (d), M489 dwarf (e), and M489 + GA3 (f). Cell files giving rise to stomatal complexes in the region 2 to 5 mm from the ligule are depicted in g through i. CMTs were randomly aligned in the interstomatal cells of both wild type (g and h) and M489 (i). In the basal EZ, stomatal mother cells were starting to form dense central MT bands (small arrows), whereas the CMTs of two lateral cells were starting to form PPBs (large arrows). In a slightly older region, MT bands (arrows) in the stomatal mother cells and PPBs of two lateral cells were well formed (h). In M489 (i) an interstomatal cell with randomized CMTs separates developing stomatal complexes consisting of guard mother cells and flanking subsidiary cells. All bars = 10 μm. All micrographs show cells aligned with their axis of elongation approximately parallel to the longitudinal axis of the page.

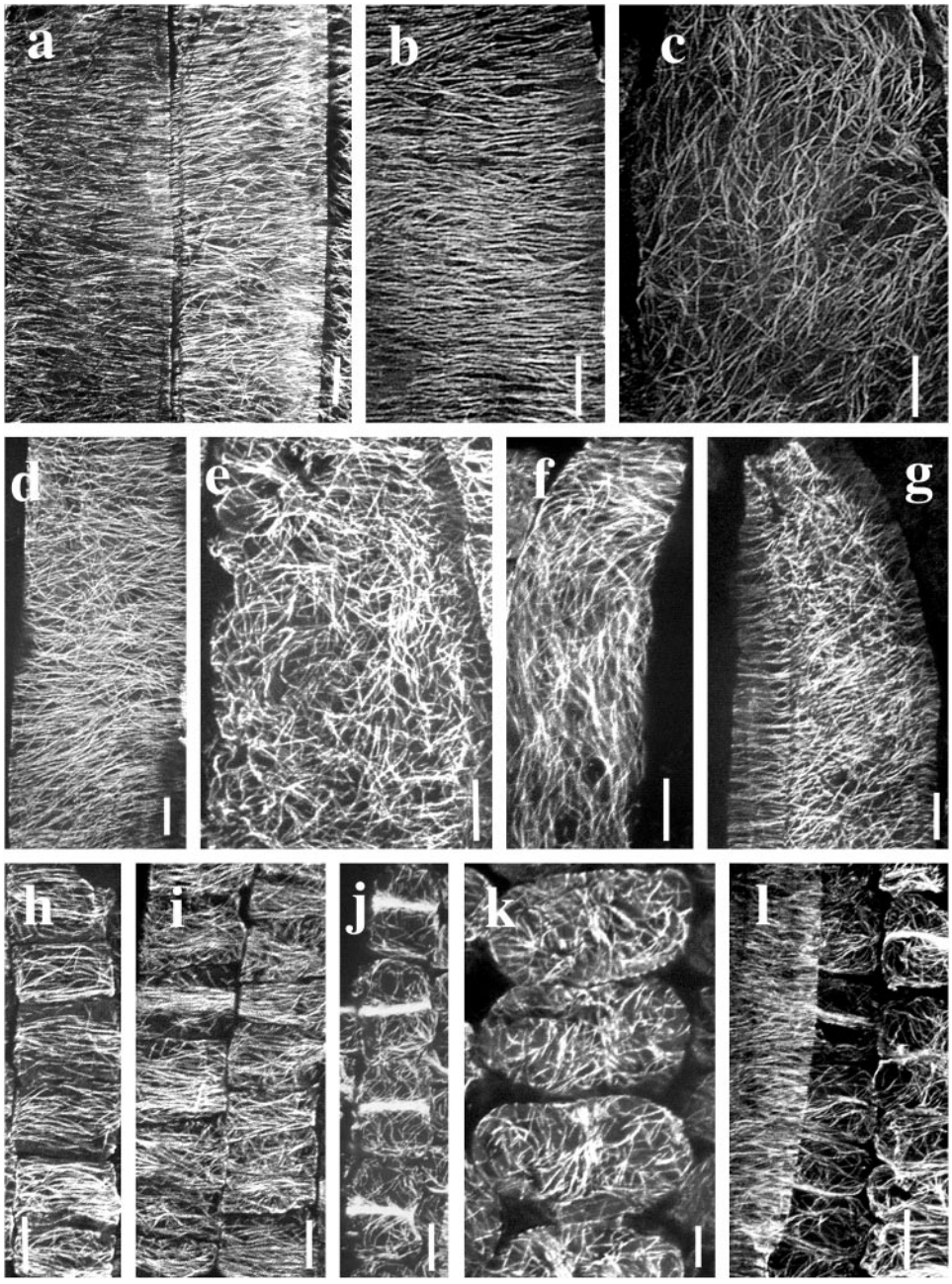

Figure 6. Confocal projections of immunofluorescently labeled microtubules in epidermal cells of the distal EZ (a–g) and mesophyll tissue (h–l). CMTs were predominantly transverse in 90% of epidermal cells of the wild-type distal EZ, 10 to 15 mm from ligule including these adaxial epidermal cells lying over a vein (a). CMTs were also predominantly transverse in epidermal cells of M489 + GA_3, 2 to 5 mm from ligule (b), but randomly oriented in a few cells in the same region (c). Both b and c depict between the veins (*bv*) abaxial cells. In the distal EZ of the M489 dwarf (5–10 mm from ligule), CMT orientations ranged from loosely transverse (d) to randomized (e). Both d and e are from *bv* (abaxial) cells. CMT orientations were sometimes variable within individual cells. In an epidermal cell from M489 + GA_3 (2–5 mm from ligule), CMT orientation shifts from transverse to longitudinal (f). In the 489 dwarf, (5–10 mm from ligule), an artifactually flattened abaxial epidermal cell has randomly oriented CMTs along the outer periclinal wall and transversely oriented CMTs along the anticlinal walls (g). Mesophyll cell development and CMT patterns were the same in dwarf and tall barley leaves. In the meristematic zone, 1 to 2 mm from ligule, CMTs were predominantly transverse in both the M489 dwarf (h) and M489 + GA_3 (i). In the M489 dwarf (5–10 mm from ligule) mesophyll cells develop localized CMT bands (j) and later have randomized CMTs (k). Similar patterns were detected in the mesophyll cells of wild type (l). In this image, taken from the region 10 to 15 mm from ligule, an epidermal *bv* abaxial cell at left has transverse CMTs. Underlying mesophyll cells have mostly random CMTs except for some with localized MT bands. All bars = 10 μm. All micrographs show cells aligned with their axis of elongation approximately parallel to the longitudinal axis of the page.

GA Restricts Radial Expansion in and beyond the EZ and Promotes Overall Wall Expansion

Our study and previous reports (e.g. Tanimoto, 1987; Keyes et al., 1989; Barlow et al., 1991; Barlow, 1992; Tonkinson et al., 1995) showed that GA promotes axial elongation and restricts radial expansion. Axial promotion outweighs radial restriction so that more longitudinal cell surface is generated with GA (see also Montague, 1995). EZ length doubled to approximately 20 mm, but cells still spent about 30 h extending. GA had little effect on REGR in the basal part of the EZ, but postponed by several hours the time when REGR started to decline (after about 15 h in M489). Similar findings were reported in wheat (Paolillo et al., 1991; Tonkinson et al., 1995, 1997), although the time spent expanding was less in short wheats (Tonkinson et al., 1995, 1997). GAs increase wall extensibility in wheat (Keyes et al., 1990) and rice (Matsukura et al., 1998) leaves and suppress the peroxidase activity that reduces extensibility by promoting diferuloyl cross-linking (Fry, 1979). This may be part of the mechanism that delays the onset of declining REGR.

Within that common framework, the response differs in detail in abaxial and adaxial cells. Adaxial cells of M489 respond to GA with a 170% increase in the cell flux from the meristem. They show little change in perimeter during their passage through the EZ, but respond strongly to GA after leaving the EZ where cell perimeters increase by ≥100%. Abaxial cells show only a 70% increase in cell flux with GA, but GA restricts the increase in their perimeters even in the basal part of the EZ, whereas post-EZ changes are very small and completely suppressed by GA. The most pronounced radial expansion in the EZ occurred in its basal region as also observed in maize roots (Liang et al., 1997). Expansion of the between vein adaxial cells (often termed bulliform cells) beyond the EZ is consistent with their proposed role in leaf unrolling, which is incomplete in the EZ (Esau, 1977). Like guard cells, they may have a unique wall architecture or chemistry that enables repeated expansion and contraction.

GA Changes CMT Orientations But This May Not Cause Radial Swelling

CMT orientation was variable in the meristematic region of all material, predominantly transverse in the basal EZ of all material, but transverse in the distal EZ of tall barley where it was disordered in M489. Thus a GA response visible with the resolution of immunofluorescence was confined to the distal EZ, as seen in other studies (Blancaflor and Hasenstein, 1995a, 1995b; Ishikawa and Evans, 1995). The effect of GA_3 in stabilizing and maintaining transverse CMTs is well documented (Mita and Shibaoka, 1984b; Akashi and Shibaoka, 1987; Baluska et al., 1993; Duckett and Lloyd, 1994; Fujino et al., 1995; Mayumi and Shibaoka, 1996; Takesue and Shibaoka, 1998), but it is difficult to argue that it changes growth anisotropy in barley. First, increased radial expansion of M489 abaxial cells was measured in the basal EZ where CMTs remained transverse and indistinguishable in dwarf and tall barleys. Second, M489 adaxial cells were no wider than those of the tall barleys when they left the EZ, although their CMTs were also disordered in the distal EZ. Third, M489 supplemented with GA_3 exhibited increased anisotropy, yet maintained transverse CMTs in a smaller proportion of cells (70%–80%) compared with wild type (90%). MT responses also showed some cell specificity. Most epidermal cells in tall plants retained transverse CMTs throughout the EZ, but cells in stomatal rows did not (Fig. 5, g–i). In a similar manner, the lack of GA in the M489 dwarf did not alter mesophyll CMT patterns.

The region of high REGR in proximal regions of the EZ broadly coincided with the development of more transverse CMT orientations as noted by Baluska et al. (1993). Tall plants maintained transverse CMTs throughout the EZ, thus spanning high and declining phases of REGR, whereas M489 CMTs became disorganized before axial REGR began to decrease. Reports showing that CMT or cellulose microfibril orientations are not closely coupled to growth rates (Laskowski, 1990; Pritchard et al., 1993; Paolillo 1995; Kropf et al., 1997; Collings et al., 1998) and that GA_3, brassinolide, or auxin can reorient CMTs from longitudinal to transverse without promoting cell elongation (Sakiyama-Sogo and Shibaoka, 1993; Mayumi and Shibaoka, 1995; Takesue and Shibaoka, 1999) make it unlikely that the loss of transverse CMTs in M489 restricts REGR and so elongation.

CONCLUSIONS

GA promotes extension growth by delaying the time when REGR begins to fall. Although GA-induced changes in REGR affect all cell types, different cell types show other responses to very different degrees. Those responses include increases in cell production rates, increases in growth anisotropy, and delays in the replacement of transverse CMTs by disordered ones. Loss of CMT alignment in expanding epidermal cells of the GA-deficient dwarf was documented in line with previous findings on GA, but it seems loss of CMT alignment may not initiate increased radial growth in abaxial cells, which seems to start in cells that still have transverse CMTs.

MATERIALS AND METHODS

Plant Material and Culture Conditions

Wild-type "Himalaya" barley (*Hordeum vulgare* L. Himalaya) and the GA-responsive M489 dwarf mutant (BC_3 stocks) were used. Plants were grown in a 1:1 vermiculite: perlite mixture in 22 × 13 × 9-cm plastic boxes (approxi-

mately 15 plants/box) with a 12-h day length (approximately 400 μmol $m^{-2}s^{-1}$ photosynthetically-active radiation) and 18°C day/13°C night conditions. At seed sowing the GA_3-treated M489 plants received 500 mL/tray of aqueous 10^{-5} M GA_3 containing 100 μL of acetone to dissolve the GA_3. The control plants (M489 and wild type grown without GA_3) received 500 mL/tray of water containing 100 μL of acetone. Plants were subsequently watered daily with 50% Hoagland solution in the mornings and de-ionized water in the afternoon.

Measurement of Cell and Blade Dimensions

All measurements relate to blades of leaf one at the time they reach one-half their final length and to the fate of the cells that leave their EZ over the following 24 h. Final blade lengths were determined in preliminary experiments. The length of the first leaf blade was measured daily for about 2 weeks for five plants of each treatment. The elongation rate (v) of 50%-elongated blades was determined from the difference in average blade length for the two consecutive days between which the blade reached 50% of its final expected length. The lengths of epidermal cells between the veins (*bv*) on the adaxial and abaxial epidermis of the blade (Wenzel et al., 1997) were measured for three 50%-elongated blades for each of the dwarf and tall plants. For the tall plants, three cells of each type were measured at 1-mm intervals for the basal 10 mm (abaxial cells) or 20 mm (adaxial cells) of the blade, and then at 2-mm intervals thereafter up to 30 mm from the ligule. Cells of M489 dwarf blades were measured at 0.5-mm intervals for the basal 5 mm (abaxial cells) or 10 mm (adaxial cells) of the blade, and then at 1-mm intervals up to 20 mm from the ligule. Cell-length data was smoothed using a three-point smoothing formula such that the cell length value l_i at position z_i from the ligule was estimated as $([l_{i-1} + l_i + l_{i+1}]/3)$; a two-point smoothing formula $([l_i + l_{i+1}]/2)$ was used to estimate the first and last cell length values at the mid-position between z_i and z_{i+1}. Final cell length, l_{max}, was estimated as the average value of the last smoothed cell length in the EZ and the next four consecutive smoothed values beyond the EZ.

Smoothed cell length values were used to calculate cell flux (f, the number of cells passing a given point per unit time; $f = v/l_{max}$), cellochron (c, time taken to add a new cell to a file at the base of the EZ; $c = 1/f$), and axial REGR according to Silk et al. (1989) and Schnyder et al. (1990). REGRs were estimated using a three-point difference formula such that $REGR_i$ at position z_i from the ligule was estimated as (axial $REGR_i = f[l_{i+1} - l_{i-1}]/[z_{i+1} - z_{i-1}]$). A two-point difference formula (axial $REGR_i = f.[l_{i+1} - l_i]/[z_{i+1} - z_i]$) was used to estimate the first and last $REGR_i$ values at the mid-position between z_i and z_{i+1}. The displacement times taken to move consecutive 1-mm increments along the EZ were estimated from the axial growth trajectory (axial growth trajectory = $[v\{z\} \times t]$ + previous displacement increment), where $v(z)$ = displacement velocity at position z ($v[z] = f \times l[z]$) (Silk et al., 1989), and the time (t) was arbitrarily chosen.

Cross-sectional perimeters and surface areas of cells on the adaxial and abaxial epidermis were measured on transverse hand sections throughout the EZs of half-grown blades. Sections were taken throughout the EZ at 1, 2, 4, 6, 8, 10, 12, 14, and 16 mm from the ligule for wild type and M489 + GA_3 and at 1, 2, 3, 4, 5, 6, 7, and 8 mm for M489. Visibly collapsed or distorted cells were avoided. Cells expand radially after leaving the EZ so we determined the final dimensions of the cells that left the EZ over the 24-h period after the blade reached one-half its final length. In mature blades (i.e. about 2 weeks old) those cells extend basipetally for a distance equal to the blade extension in that 24-h period from the position of the distal end of the EZ in the half-grown leaf (i.e. from a point displaced apically from the mid-point of the mature leaf by the length of the EZ). The cross-sectional perimeters and areas of three cells of each type were measured at intervals of 2 (M489) or 4 mm (wild type and M489 + GA_3). Using the average cell perimeters from this region, longitudinal wall areas were calculated for cells and for the whole file of cells forming the 24-h growth increment. Sections were imaged on a Axioskop (Zeiss, Jena, Germany) equipped with a PCVISIONplus (Imaging Technology, Wobur, MA) frame-grabber board, and perimeters and cross-sectional areas were determined with Java video analysis software (version 1.40, Jandel Scientific, Corte Madera, CA).

Mature leaves (10 per treatment) were photocopied, and blade width was determined at 10%, 20%, 30%. . .90% positions between the ligule (0%) and the tip (100%).

Microtubule Labeling of Cells within the EZ of 50%-Elongated Blades

EZs of 50%-elongated blades were immersed in 4% (v/v) formaldehyde in 60 mM piperazine-*N*,*N*′-bis-[2-ethanesulfonic acid], 25 mM *N*-2-hydroxyethyl piperazine-*N*′-2-ethanesulfonic acid, 10 mM EGTA, 4 mM $MgSO_4$, and 5% (v/v) dimethyl sulfoxide (DMSO), pH 6.9, at room temperature (PHEM/DMSO). Successive segments (approximately 1 mm wide and 5 mm long) were cut along the EZ, vacuum-infiltrated in fixative for 5 min, and fixed overnight. Segments rinsed (3 × 5 min) in PHEM/DMSO were digested for 25 min in 2% (w/v) driselase (Sigma, St. Louis) and 1% (w/v) pectolyase (Kikkoman Corporation, Japan) in distilled water. After permeabilizing (2.5 h with 1% [v/v] Triton X-100 in PHEM/DMSO), they were rinsed (6 × 5 min) in phosphate-buffered saline (PBS) at pH 7.2.

Segments were treated overnight in a moist environment with mouse monoclonal anti-β tubulin (product N357, Amersham, Buckinghamshire, UK) diluted 1:500, rinsed (6 × 5 min) in PBS, and incubated for 4 h in fluorescein isothiocyanate-conjugated sheep anti-mouse Ig F(ab′)2 fragment (Silenus/Amrad Biotech, Boronia, Victoria, Australia) diluted 1:30. Antibodies were diluted in PBS with 1% (w/v) bovine serum albumin and 0.02% (w/v) NaN_3. Segments rinsed in PBS (6 × 5 min) were mounted in 0.1% (w/v) para-phenylene diamine in 1:1 glycerol:PBS at pH 9 to 9.5. Samples were stored in the dark at 4°C until examined. For each treatment, at least five tissue segments taken at each distance (0–5, 5–10 mm, etc. from the ligule) were examined from ≥10 leaves.

Tissue was examined with a confocal laser scanning system (MRC-Bio-Rad 600, Microscience Division, Hemel, Hempstead, UK) coupled to an Axiovert IM-10 (Zeiss) with ArKr laser, BHS filter block, and oil immersion objectives. Images were recorded using COMOS software, projections generated with Confocal Assistant (version 4.02, Todd Clarke Brelje), and images processed in Adobe Photoshop 4.0 (Adobe Systems, Mountain View, CA).

ACKNOWLEDGMENTS

We thank P.M. Chandler for barley lines; P.M. Chandler, J.B. Passioura, and W. Silk for helpful discussions; A.L. Cleary for assistance with the MT labeling technique; and S. Stowe and D. Vowles for help with the morphometric analyses.

Received March 14, 2000; accepted June 23, 2000.

LITERATURE CITED

Akashi T, Shibaoka H (1987) Effects of gibberellin on the arrangement and the cold stability of cortical microtubules in epidermal cells of pea internodes. Plant Cell Physiol **28:** 339–348

Baluska F, Parker JS, Barlow PW (1993) A role for gibberellic acid in orienting microtubules and regulating cell growth polarity in the maize root cortex. Planta **191:** 149–157

Barlow PW (1992) The meristem and quiescent center in cultured root apices of the *gib-1* mutant of tomato (*Lycopersicon esculentum* Mill.). Ann Bot **69:** 533–543

Barlow PW, Brain P, Parker JS (1991) Cellular growth in roots of a gibberellin-deficient mutant of tomato (*Lycopersicon esculentum* Mill.) and its wild type. J Exp Bot **42:** 339–351

Baskin TI, Betzner AS, Hoggart R, Cork A, Williamson RE (1992) Root morphology mutants in *Arabidopsis thaliana*. Aust J Plant Physiol **19:** 427–437

Blancaflor EB, Hasenstein KH (1995a) Growth and microtubule orientation of *Zea mays* roots subjected to osmotic stress. Intl J Plant Sci **156:** 774–783

Blancaflor EB, Hasenstein KH (1995b) Time course and auxin sensitivity of cortical microtubule reorientation in maize roots. Protoplasma **185:** 72–82

Chandler PM, Robertson M (1999) Gibberellin dose-response curves and the characterization of dwarf mutants of barley. Plant Physiol **120:** 623–632

Collings DA, Winter H, Wyatt SE, Allen NS (1998) Growth dynamics and cytoskeleton organization during stem maturation and gravity-induced stem bending in *Zea mays* L. Planta **207:** 246–258

Duckett CM, Lloyd CW (1994) Gibberellic acid-induced microtubule reorientation in dwarf peas is accompanied by rapid modification of an α-tubulin isotype. Plant J **5:** 363–372

Durnam DJ, Jones RL (1982) The effects of colchicine and gibberellic acid on growth and microtubules in excised lettuce hypocotyls. Planta **154:** 204–211

Esau K (1977) Anatomy of Seed Plants, Ed 2. John Wiley & Sons, New York

Fry SC (1979) Phenolic components of the primary cell wall and their possible role in the hormonal regulation of growth. Planta **146:** 343–351

Fujino K, Koda Y, Kikuta Y (1995) Reorientation of cortical microtubules in the sub-apical region during tuberization in single-node stem segments of potato in culture. Plant Cell Physiol **36:** 891–895

Giddings TH Jr, Staehelin LA (1988) Spatial relationship between microtubules and plasma-membrane rosettes during the deposition of primary wall microfibrils in *Closterium* sp. Planta **173:** 22–30

Giddings TH Jr, Staehelin LA (1991) Microtubule-mediated control of microfibril deposition: a re-examination of the hypothesis. *In* CW Lloyd, ed, The Cytoskeletal Basis of Plant Growth and Form. Academic Press, London, pp 85–99

Hauser M-T, Morikami A, Benfey PN (1995) Conditional root expansion mutants of *Arabidopsis.* Development **121:** 1237–1252

Hellmann A, Wernicke W (1998) Changes in tubulin protein expression accompany reorganization of microtubular arrays during cell shaping in barley leaves. Planta **204:** 220–225

Ishikawa H, Evans ML (1995) Specialized zones of development in roots. Plant Physiol **109:** 725–727

Keyes GJ, Paolillo DJ, Sorrells ME (1989) The effects of dwarfing genes *Rht1* and *Rht2* on cellular dimensions and rate of leaf elongation in wheat. Ann Bot **64:** 683–690

Keyes G, Sorrells ME, Setter TL (1990) Gibberellic acid regulates cell wall extensibility in wheat (*Triticum aestivum* L.). Plant Physiol **92:** 242–245

Kropf DL, Bisgrove SR, Hable WE (1998) Cytoskeletal control of polar growth in plant cells. Curr Opin Cell Biol **10:** 117–122

Kropf DL, Williamson RE, Wasteneys GO (1997) Microtubule orientation and dynamics in elongating characean internodal cells following cytosolic acidification, induction of pH bands, or premature growth arrest. Protoplasma **197:** 188–198

Laskowski MJ (1990) Microtubule orientation in pea stem cells: a change in orientation follows the initiation of growth rate decline. Planta **181:** 44–52

Liang BM, Sharp RE, Baskin TI (1997) Regulation of growth anisotropy in well-watered and water-stressed maize roots: I. Spatial distribution of longitudinal, radial, and tangential expansion rates. Plant Physiol **115:** 101–111

Matsukura C, Itoh S-I, Nemoto K, Tanimoto E, Yamaguchi J (1998) Promotion of leaf sheath growth by gibberellic acid in a dwarf mutant of rice. Planta **205:** 145–152

Mayumi K, Shibaoka H (1995) A possible double role for brassinolide in the reorientation of cortical microtubules in the epidermal cells of azuki bean epicotyls. Plant Cell Physiol **36:** 173–181

Mayumi K, Shibaoka H (1996) The cyclic reorientation of cortical microtubules on walls with a crossed polylamellate structure: effects of plant hormones and an inhibitor

of protein kinases on the progression of the cycle. Protoplasma **195:** 112–122

Mita T, Katsumi M (1986) Gibberellin control of microtubule arrangement in the mesocotyl epidermal cells of the d_5 mutant of *Zea mays* L. Plant Cell Physiol **27:** 651–659

Mita T, Shibaoka H (1983) Changes in microtubules in onion leaf sheath cells during bulb development. Plant Cell Physiol **24:** 109–117

Mita T, Shibaoka H (1984a) Effects of S-3307, an inhibitor of gibberellin biosynthesis, on swelling of leaf sheath cells and on the arrangement of cortical microtubules in onion seedlings. Plant Cell Physiol **25:** 1531–1539

Mita T, Shibaoka H (1984b) Gibberellin stabilizes microtubules in onion leaf sheath cells. Protoplasma **119:** 100–109

Montague MJ (1995) Gibberellic acid promotes growth and cell wall synthesis in *Avena* internodes regardless of the orientation of cell expansion. Physiol Plant **94:** 7–18

Murata T, Wada M (1989) Effects of colchicine and amiprophos-methyl on microfibril arrangement and cell shape in *Adiantum* protonemal cells. Protoplasma **151:** 81–87

Paolillo DJ Jr (1995) The net orientation of wall microfibrils in the outer periclinal epidermal walls of seedling leaves of wheat. Ann Bot **76:** 589–596

Paolillo DJ Jr, Sorrells ME, Keyes GJ (1991) Gibberellic acid sensitivity determines the length of the extension zone in wheat leaves. Ann Bot **67:** 479–485

Pritchard J, Hetherington PR, Fry SC, Deri Tomos A (1993) Xyloglucan endotransglycosylase activity microfibril orientation and the profiles of cell wall properties along growing regions of maize roots. J Exp Bot **44:** 1281–1289

Sakiyama-Sogo M, Shibaoka H (1993) Gibberellin A_3 and abscisic acid cause the reorientation of cortical microtubules in epicotyl cells of the decapitated dwarf pea. Plant Cell Physiol **34:** 431–437

Schnyder H, Seo S, Rademacher IF, Kuhbauch W (1990) Spatial distribution of growth rates and of epidermal cell lengths in the elongation zone during leaf development in *Lolium perenne* L. Planta **181:** 423–431

Shibaoka H (1993) Regulation by gibberellins of the orientation of cortical microtubules in plant cells. Aust J Plant Physiol **20:** 461–470

Silk WK, Lord EM, Eckard KJ (1989) Growth patterns inferred from anatomical records: empirical tests using longisections of roots of *Zea mays* L. Plant Physiol **90:** 708–713

Srivastava LM, Sawhney VK, Bonettemaker M (1977) Cell growth, wall deposition, and correlated fine structure of colchicine-treated lettuce hypocotyl cells. Can J Bot **55:** 902–917

Takesue K, Shibaoka H (1998) The cyclic reorientation of cortical microtubules in epidermal cells of azuki bean epicotyls: the role of actin filaments in the progression of the cycle. Planta **205:** 539–546

Takesue K, Shibaoka H (1999) Auxin-induced longitudinal-to-transverse reorientation of cortical microtubules in nonelongating epidermal cells of azuki bean epicotyls. Protoplasma **206:** 27–30

Tanimoto E (1987) Gibberellin-dependent root elongation in *Lactuca sativa*: recovery from growth retardant-suppressed elongation with thickening by low concentration of GA_3. Plant Cell Physiol **28:** 963–973

Tonkinson CL, Lyndon RF, Arnold GM, Lenton JR (1995) Effect of the *Rht3* dwarfing gene on dynamics of cell extension in wheat leaves, and its modification by gibberellic acid and paclobutrazol. J Exp Bot **46:** 1085–1092

Tonkinson CL, Lyndon RF, Arnold GM, Lenton JR (1997) The effects of temperature and the *Rht3* dwarfing gene on growth, cell extension, and gibberellin content and responsiveness in the wheat leaf. J Exp Bot **48:** 963–970

Veen BW (1982) The influence of mechanical impedance on the growth of maize roots. Plant Soil **66:** 101–109

Wasteneys GO (1992) The Characean cytoskeleton: spatial control in the cortical cytoplasm. *In* D Menzel, ed, The Cytoskeleton of the Algae. CRC Press, Boca Raton, FL, pp 273–295

Wenzel CL (1998) Leaf epidermal cell dynamics of barley (*Hordeum vulgare* L., "Himalaya") and some stature mutants. PhD thesis. Australian National University, Canberra, Australia

Wenzel CL, Chandler PM, Cunningham RB, Passioura JB (1997) Characterization of the leaf epidermis of barley (*Hordeum vulgare* L. "Himalaya"). Ann Bot **79:** 41–46